

Geometric k-essence and late-time acceleration from integrable nonmetricity

Lehel Csillag

September 2, 2025



Joint work with Erik Jensko

- ① Geometrical preliminaries**
- ② Geometric k-essence**
- ③ Cosmological dynamics of geometric k-essence**
- ④ Late-time observational constraints**
- ⑤ Outlook**

- ① Geometrical preliminaries**
- ② Geometric k-essence**
- ③ Cosmological dynamics of geometric k-essence**
- ④ Late-time observational constraints**
- ⑤ Outlook**

Fundamental objects of non-Riemannian geometry

A general affine connection is fully characterized by its torsion and nonmetricity

$$Q_{\mu\nu\rho} = -\nabla_\mu g_{\nu\rho}, \quad T^\mu{}_{\nu\rho} = \Gamma^\mu{}_{\rho\nu} - \Gamma^\mu{}_{\nu\rho}.$$

With the help of these, the affine connection can be decomposed as

$$\Gamma^\mu{}_{\nu\rho} = \overset{\circ}{\Gamma}{}^\mu{}_{\nu\rho} + \frac{1}{2}g^{\mu\lambda}(Q_{\nu\rho\lambda} + Q_{\rho\lambda\nu} - Q_{\lambda\nu\rho}) - \frac{1}{2}g^{\mu\lambda}(T_{\rho\nu\lambda} - T_{\lambda\rho\nu} + T_{\nu\rho\lambda}).$$

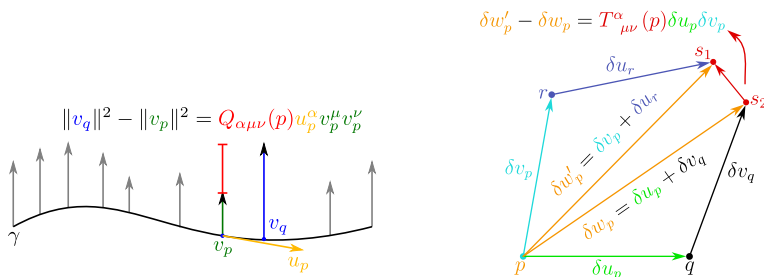
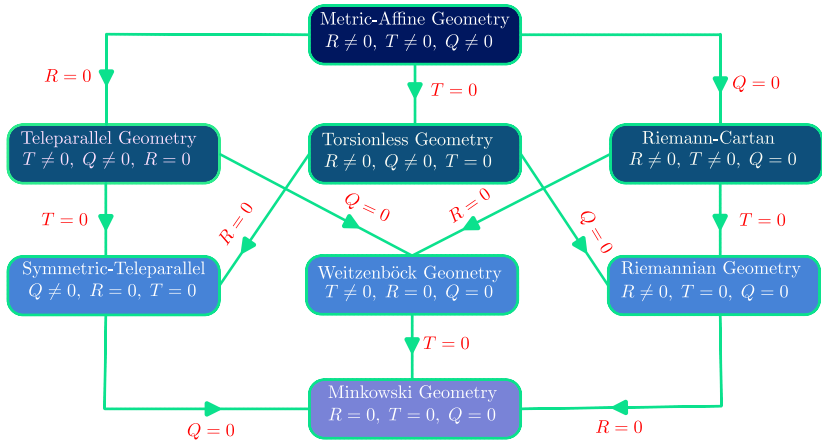


Figure 1: The effects of nonmetricity (left panel) and torsion (right panel) are depicted. nonmetricity changes the lengths of vectors, while torsion measures to what extent the parallelogram law fails infinitesimally.

Landscape of non-Riemannian geometries



For a connection with vectorial nonmetricity, $Q_{\mu\nu\rho}$ takes the form

$$Q_{\mu\nu\rho} = c_1 \pi_\mu g_{\nu\rho} + c_2 (\pi_\rho g_{\mu\nu} + \pi_\nu g_{\rho\mu}) + 2c_3 \pi_\mu \pi_\nu \pi_\rho.$$

This extends many historical works in the literature:

- Weyl geometric framework: c_1 associated with scale invariance (Weyl, 1918)
- Generalized Weyl nonmetricity: adds c_2 terms (Aringazin, Mikhailov, 1991)
- Linear vectorial distortion: include c_1 and c_2 plus linear torsion terms (Jiménez and Koivisto, 2016)

Remark: The c_3 term is completely symmetric, reminiscent to the cubic tensor of statistical manifolds.

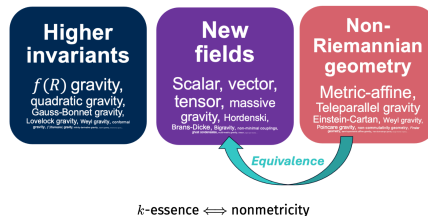
Why this form of nonmetricity?

- On FLRW backgrounds the most general form of nonmetricity (Iosifidis 2003.07384) takes the form

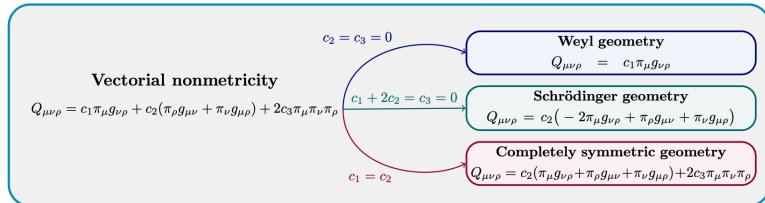
$$Q_{\mu\nu\rho} = A(t)u_\mu h_{\nu\rho} + B(t)(u_\rho h_{\mu\nu} + \pi_\nu g_{\mu\rho}) + 2C(t)u_\mu u_\nu u_\rho,$$

where A , B and C are arbitrary functions of time.

- Reduces exactly to our form in the simple case $A \propto B \propto C$.
- 'Natural' extension (all allowed terms without contractions $\pi_\mu \pi^\mu$).
- Phenomenological reasons: the new c_3 term plays a key role in describing dark energy in cosmology.



Vectorial nonmetricity and its special cases



We introduce the dilation Q_μ and shear $\bar{Q}_{\mu\nu\rho}$,

$$Q_{\mu\nu\rho} = Q_\mu g_{\nu\rho} + \bar{Q}_{\mu\nu\rho}, \text{ where } Q_\mu = Q_{\mu\nu}{}^\lambda / 4, \quad \bar{Q}_{\mu\lambda} = 0.$$

Geometry	Dilation	Shear
Weyl	π_μ	0
Schrödinger	$-\frac{3}{2}c_2 \pi_\mu$	$c_2 \pi_\rho g_{\mu\nu} + c_2 \pi_\nu g_{\rho\mu} - \frac{c_2}{2} \pi_\mu g_{\nu\rho}$
Completely symmetric	$\frac{3c_2}{2} \pi_\mu + \frac{c_3}{2} \pi_\mu \pi_\lambda \pi^\lambda$	$c_2 \pi_\rho g_{\mu\nu} + c_2 \pi_\nu g_{\rho\mu} + 2c_3 \pi_\mu \pi_\nu \pi_\rho - \frac{c_2}{2} \pi_\mu g_{\nu\rho} - \frac{c_3}{2} g_{\nu\rho} \pi_\mu \pi_\lambda \pi^\lambda$

Theorem 1.1. Length preservation

Let ∇ be a connection with vectorial nonmetricity. Then, for all vector fields, which satisfy $\nabla_X X = 0$, the following are equivalent:

- (i) ∇ preserves lengths under parallel transport, i.e. $\nabla_X(g(X, X)) = 0$.
- (ii) The coefficients of the vectorial nonmetricity satisfy $c_1 = -2c_2$, $c_3 = 0$.

Theorem 1.2. Angle preservation

For a connection ∇ with vectorial nonmetricity, the following are equivalent:

- (i) ∇ preserves angles under parallel transport, that is,

$$\frac{|g(X, Y)|}{\sqrt{|g(X, X)|} \sqrt{|g(Y, Y)|}} = \frac{|(\nabla_Z g)(X, Y)|}{\sqrt{|(\nabla_Z g)(X, X)|} \sqrt{|(\nabla_Z g)(Y, Y)|}}.$$

- (ii) The coefficients of the vectorial nonmetricity satisfy $c_2 = c_3 = 0$.

Ricci tensor

$$\begin{aligned}
 R_{\mu\nu} = & \overset{\circ}{R}_{\mu\nu} + \overset{\circ}{\nabla}_\nu \pi_\mu \left(-\frac{3c_1}{2} - c_2 \right) + \frac{c_1}{2} \overset{\circ}{\nabla}_\mu \pi_\nu + c_3 \left(\overset{\circ}{\nabla}_\rho (\pi^\rho \pi_\nu \pi_\mu) - \overset{\circ}{\nabla}_\nu (\pi^\rho \pi_\rho \pi_\mu) \right) \\
 & + \pi_\mu \pi_\nu \left(-\frac{c_1^2}{4} - \frac{c_1 c_3}{2} \pi^\beta \pi_\beta + c_1^2 + 2c_1 c_3 \pi^\beta \pi_\beta - \frac{(2c_2 - c_1)^2}{4} - \frac{2c_2 - c_1}{2} c_3 \pi^\beta \pi_\beta \right) \\
 & + \frac{2c_2 - c_1}{2} g_{\mu\nu} \left(\overset{\circ}{\nabla}_\rho \pi^\rho + c_2 \pi^\rho \pi_\rho + 2c_1 \pi_\beta \pi^\beta + c_3 \pi_\beta \pi^\beta \pi^\rho \pi_\rho - \frac{c_1}{2} \pi^\rho \pi_\rho - \frac{c_1}{2} \pi^\beta \pi_\beta \right)
 \end{aligned}$$

Note that $R_{\mu\nu} \neq R_{(\mu\nu)}$!

Ricci scalar

$$R = \overset{\circ}{R} - \frac{3}{2} c_1^2 \pi_\mu \pi^\mu + 3c_1 c_2 \pi_\mu \pi^\mu + 3c_2^2 \pi_\mu \pi^\mu + 3c_2 c_3 \pi_\mu \pi^\mu \pi_\lambda \pi^\lambda - 3c_1 \overset{\circ}{\nabla}_\mu \pi^\mu + 3c_2 \overset{\circ}{\nabla}_\mu \pi^\mu$$

① Geometrical preliminaries

② Geometric k-essence

③ Cosmological dynamics of geometric k-essence

④ Late-time observational constraints

⑤ Outlook

Quintessence

$$S[g, \phi, \psi] = \int d^4x \sqrt{-g} \left[\overset{\circ}{R} - \frac{1}{2} g^{\mu\nu} \partial_\mu \phi \partial_\nu \phi - V(\phi) \right] + S_m[g, \psi].$$

K-essence

$$S[g, \phi, \psi] = \int d^4x \sqrt{-g} \left[\overset{\circ}{R} + K(\phi, X) \right] + S_m[g, \psi], \quad X = -\frac{1}{2} g^{\mu\nu} \partial_\mu \phi \partial_\nu \phi.$$

They are related by

$$K(\phi, X) = X - V(\phi).$$

Purely kinetic k-essence: $K(\phi, X) = K(X)$ – absence of potential.

Causality conditions for a healthy theory

$$K_X := \frac{dK(X)}{dX} \geq 0, \quad K_{XX} := \frac{d^2K(X)}{dx^2} \geq 0.$$

Advantages over quintessence

Feature	Advantage of K-essence
Kinetic structure	Non-canonical kinetic term: richer dynamics.
Sound speed	Variable sound speed $c_s^2 \neq 1$ affects structure growth; quintessence has $c_s^2 = 1$.
Unified framework	Can describe both inflation and dark energy in a single scalar field model.
Phantom crossing	Can access $w < -1$ regime without ghosts, unlike quintessence.

Action principle for vectorial nonmetricity

We propose the action

$$S[g, \pi, \phi, \lambda, \psi] = \frac{1}{2\kappa} \int \sqrt{-g} (R + \xi \nabla_\mu \pi^\mu) d^4x + S_\lambda[g, \pi, \phi, \lambda] + S_m[g, \psi],$$

where the Ricci scalar is given by

$$R = \overset{\circ}{R} - \frac{3}{2} c_1^2 \pi^\mu \pi_\mu + 3c_1 c_2 \pi_\mu \pi^\mu + 3c_2^2 \pi_\mu \pi^\mu + 3c_2 c_3 \pi_\mu \pi^\mu \pi_\lambda \pi^\lambda - 3c_1 \overset{\circ}{\nabla}_\mu \pi^\mu + 3c_2 \overset{\circ}{\nabla}_\mu \pi^\mu.$$

The field equations obtained from the variational principle read

$$\begin{aligned} \overset{\circ}{G}_{\mu\nu} + \overset{\circ}{\nabla}_\mu \phi \overset{\circ}{\nabla}_\nu \phi \left(b_1 + b_2 \overset{\circ}{\nabla}_\lambda \phi \overset{\circ}{\nabla}^\lambda \phi \right) - \frac{1}{2} g_{\mu\nu} \overset{\circ}{\nabla}_\lambda \phi \overset{\circ}{\nabla}^\lambda \phi \left(b_1 + \frac{b_2}{2} \overset{\circ}{\nabla}_\rho \phi \overset{\circ}{\nabla}^\rho \phi \right) &= \kappa T_{\mu\nu}, \\ b_1 \overset{\circ}{\nabla}_\mu \overset{\circ}{\nabla}^\mu \phi + b_2 \left(\overset{\circ}{\nabla}_\mu \phi \overset{\circ}{\nabla}^\mu \phi \overset{\circ}{\nabla}_\nu \overset{\circ}{\nabla}^\nu \phi + 2 \overset{\circ}{\nabla}_\mu \phi \overset{\circ}{\nabla}^\nu \phi \overset{\circ}{\nabla}_\nu \overset{\circ}{\nabla}^\mu \phi \right) &= 0, \end{aligned}$$

where the following two constants parameterise the whole theory

$$b_1 = -\frac{3c_1^2}{2} + c_2(3c_2 + \xi) + c_1(3c_2 + 2\xi), \quad b_2 = 2c_3(3c_2 + \xi).$$

With b_1, b_2 and $b_3 = -3c_1 + 3c_2 + \xi$, we have

$$R + \xi \nabla_\mu \pi^\mu = \overset{\circ}{R} + b_1 \overset{\circ}{\nabla}{}^\mu \phi \overset{\circ}{\nabla}_\mu \phi + \frac{1}{2} b_2 \overset{\circ}{\nabla}{}^\mu \phi \overset{\circ}{\nabla}_\mu \phi \overset{\circ}{\nabla}{}^\nu \phi \overset{\circ}{\nabla}_\nu \phi + \textcolor{blue}{b_3 \overset{\circ}{\nabla}_\mu \overset{\circ}{\nabla}{}^\mu \phi},$$

where the **blue term** is a boundary term.

The key identification

$$\mathcal{L} = \frac{1}{2} \overset{\circ}{R} + \mathcal{L}_K, \quad \mathcal{L}_K = K(\phi, X) = -b_1 X + b_2 X^2, \quad X = -\frac{1}{2} \overset{\circ}{\nabla}{}^\mu \phi \overset{\circ}{\nabla}_\mu \phi.$$

- **Equation of state**

$$w_\phi = \frac{P}{\rho_\phi} = \frac{P}{2XP_{,X} - P} = \frac{b_1 - b_2 X}{b_1 - 3b_2 X},$$

- **Adiabatic sound speed squared**

$$c_s^2 = \frac{P_{,X}}{\rho_{\phi,X}} = \frac{b_1 - 2b_2 X}{b_1 - 6b_2 X} = \frac{1 + w_\phi}{5 - 3w_\phi}.$$

- **Weyl geometry** with $c_2 = c_3 = 0$ and arbitrary ξ gives

$$b_1 = -\frac{3c_1^2}{2} + 2c_1\xi, \quad b_2 = 0.$$

The kinetic term in the action has the correct (negative) sign if either $c_1 > 0$ and $4\xi < 3c_1$, or if $c_1 < 0$ and $4\xi > 3c_1$. The theory is mapped to standard gravity minimally coupled to a canonical scalar field ($b_1 = -1/2$) with vanishing potential when $\xi = (3c_1^2 - 1)/4c_1$.

- **Schrödinger geometry** with $c_1 = -2c_2$, $c_3 = 0$ and $\xi = 0$ gives

$$b_1 = -9c_2^2, \quad b_2 = 0.$$

The parameter b_1 is always negative and the kinetic term therefore always has the correct sign.

- **Completely symmetric geometry** with $c_1 = c_2$ and $\xi = 0$ gives

$$b_1 = \frac{9c_2^2}{2}, \quad b_2 = 6c_2c_3.$$

In this case, both b_1 and b_2 are generally non-zero. The coefficient b_1 is always positive, whereas b_2 can take either sign depending on the parameters.

- ① Geometrical preliminaries
- ② Geometric k-essence
- ③ Cosmological dynamics of geometric k-essence
- ④ Late-time observational constraints
- ⑤ Outlook

The Friedmann equations

$$\begin{aligned}3H^2 &= \kappa\rho - \frac{1}{2}b_1\varphi^2 + \frac{3}{4}b_2\varphi^4, \\3H^2 + 2\dot{H} &= -\kappa\rho + \frac{1}{2}b_1\varphi^2 - \frac{1}{4}b_2\varphi^4, \\b_1(3H\varphi + \dot{\varphi}) &= b_2(3H\varphi^3 + 3\varphi^2\dot{\varphi}).\end{aligned}$$

can be rewritten using the dynamical variables

$$\Omega_m = \frac{\kappa\rho}{3H^2}, \quad x = -\frac{b_1\varphi^2}{6H^2}, \quad y = \frac{b_2\varphi^4}{4H^2}$$

in the following form

$$\begin{aligned}\frac{dx}{dN} &= x\left(3x + y + 1 + 3w(1 - x - y) - \frac{4x}{x + 2y}\right), \\\frac{dy}{dN} &= y\left(3x + y - 1 + 3w(1 - x - y) - \frac{8x}{x + 2y}\right).\end{aligned}$$

We also find a simple relation

$$\frac{1}{x} \frac{dx}{dN} - \frac{1}{y} \frac{dy}{dN} = \frac{6x + 4y}{x + 2y}.$$

Stability constraints and fixed points

The sound speed squared and EoS parameter are

$$w_\phi = \frac{3x+y}{3(x+y)}, \quad c_s^2 = \frac{1}{3} + \frac{2x}{3(x+2y)}, \quad w_{\text{eff}} = w_\phi \Omega_\phi + w \Omega_m.$$

The deceleration parameter is given by

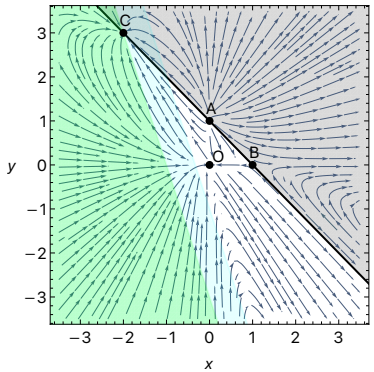
$$q := -\frac{\dot{H}}{H^2} - 1 = \frac{1}{2}(1 + 3x + y + 3w\Omega_m).$$

For linear stability, we study the eigenvalues of

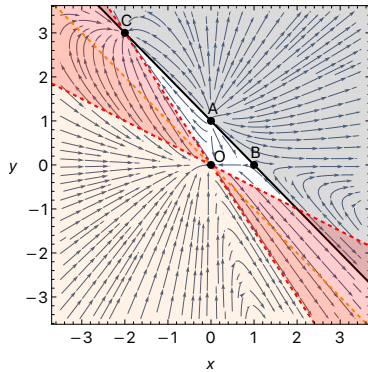
$$J(x_*, y_*) = \left(\begin{array}{cc} \frac{\partial f_1}{\partial x} & \frac{\partial f_1}{\partial y} \\ \frac{\partial f_2}{\partial x} & \frac{\partial f_2}{\partial y} \end{array} \right) \Bigg|_{(x,y)=(x_*,y_*)}.$$

Point	Ω_m	x	y	w_{eff}	c_s^2	stability	conditions
A	0	0	1	$\frac{1}{3}$	$\frac{1}{3}$	unstable	$b_2 > 0$
B	0	1	0	1	1	saddle	$b_1 < 0$
C	0	-2	3	-1	0	stable	$b_1 > 0 \text{ \& } b_2 > 0$
O	1	0	0	w	-	-	none

Phase portraits



(a) Phase space showing accelerated expansion $-1 \leq w_{\text{eff}} \leq -1/3$ (blue) and phantom regime $w_{\text{eff}} < -1$ (green).



(b) Phase space showing stability conditions. Red region (red dashed border) indicates $c_s^2 < 0$ and orange region (orange dashed border) indicates $\rho_\phi < 0$.

Evolution plots

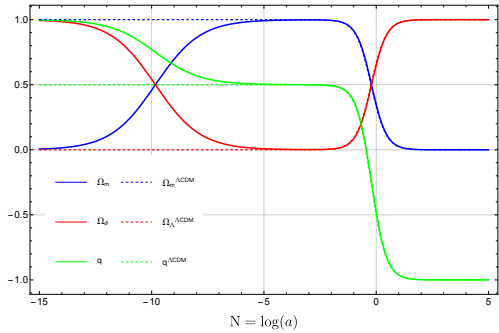


Figure 3: Evolution of the matter density parameter Ω_m , the k -essence density parameter Ω_ϕ , and the deceleration parameter q in the geometric k -essence model, compared to the standard Λ CDM scenario.

- ① Geometrical preliminaries
- ② Geometric k-essence
- ③ Cosmological dynamics of geometric k-essence
- ④ Late-time observational constraints**
- ⑤ Outlook

Dimensionless and redshift representations

We introduce a set of dimensionless variables (h, τ, r, Φ, B) as

$$h = \frac{H}{H_0}, \quad \tau = H_0 t, \quad r = \frac{\rho \kappa}{3H_0^2}, \quad \Phi = \frac{\sqrt{b_1} \varphi}{H_0}, \quad B = \frac{3b_2 H_0^2}{4b_1^2}.$$

The Friedmann equations with $p = 0$ take the form

$$3h^2 = 3r - \frac{1}{2}\Phi^2 + B\Phi^4,$$

$$3h^2 + 2\frac{dh}{d\tau} = \frac{1}{2}\Phi^2 - \frac{1}{3}B\Phi^4,$$

$$\frac{d\Phi}{d\tau} + 3h\Phi = 4B\left(\frac{d\Phi}{d\tau}\Phi^2 + h\Phi^3\right).$$

In the redshift representation with $1+z = 1/a$, they read

$$3h(z)^2 = 3r(z) - \frac{1}{2}\Phi(z)^2 + B\Phi(z)^4,$$

$$\frac{dh(z)}{dz} = \frac{3h(z)^2 - \frac{1}{2}\Phi(z)^2 + \frac{1}{3}B\Phi(z)^4}{2(1+z)h(z)},$$

$$\frac{d\Phi(z)}{dz} = \frac{-4Bh(z)\Phi(z)^3 + 3h(z)\Phi(z)}{(1+z)h(z)(1-4B\Phi^2)}.$$

Approaches to solving the equations

- Solve the equations numerically for $\Phi(z)$, $h(z)$, and obtain Ω_m from Friedmann constraint.
- Use the continuity equation to write the matter density parameter explicitly in terms of $\Omega_{m0}(1+z)^3$, and use the scalar field equation to get an integral expression for Φ to use in the Friedmann constraint.

The present day matter density and Φ_0 are related through

$$1 = \Omega_{m0} - \frac{1}{6}\Phi_0^2 + \frac{B}{3}\Phi_0^4,$$

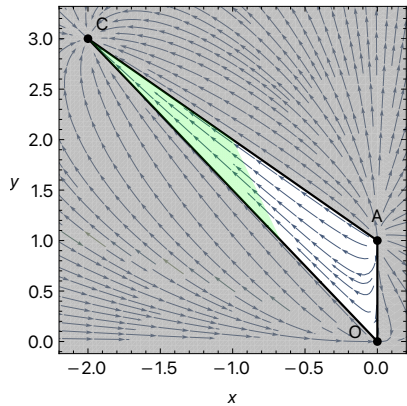
The positive energy $\Omega_m \geq 0$, $\rho_\phi \geq 0$ and perturbative stability condition yield

$$0 \leq \Omega_{m0} \leq 1, \quad B \geq \frac{1}{16 - 16\Omega_{m0}}.$$

In addition, assuming that the Universe is accelerating today, we get the bounded region

$$0 \leq \Omega_{m0} < 2/3, \quad \frac{1}{16 - 16\Omega_{m0}} \leq B < \frac{4 - 3\Omega_{m0}}{6(\Omega_{m0} - 2)^2}.$$

Allowed parameter region

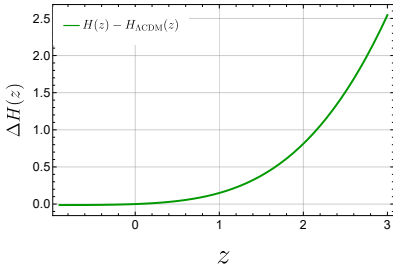
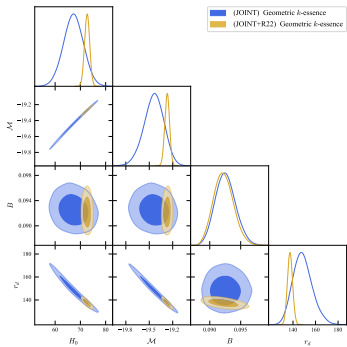


Steps:

- Impose $0 \leq \Omega_m \leq 1$ and $c_s^2 \geq 0$
- Trajectories do not cross $x = 0$, so consider only negative values of x (positive values of b_1) for existence of de Sitter points
- Observe that trajectories inside this region remain bounded and pathology-free for all time

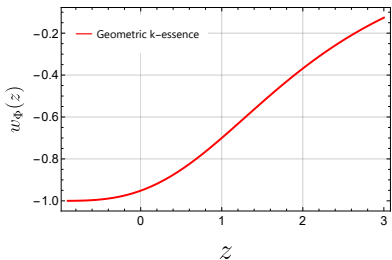
Inferred parameters and their contours

Cosmological Model	Parameter	Prior	JOINT	JOINT + R22
Λ CDM	H_0	[50, 100]	67.3 ± 3.9	72.7 ± 1.0
	Ω_{m0}	[0, 1]	0.324 ± 0.012	0.322 ± 0.012
	\mathcal{M}	[-20, -18]	$-19.44^{+0.13}_{-0.12}$	-19.271 ± 0.030
	r_d	[100, 300]	$148.6^{+7.5}_{-9.5}$	137.4 ± 2.3
Geometric k -essence	H_0	[50, 100]	67.3 ± 3.9	72.7 ± 1.0
	B	[0.0880, 0.1784]	$0.0925^{+0.0015}_{-0.0018}$	$0.0922^{+0.0015}_{-0.0017}$
	\mathcal{M}	[-20, -18]	$-19.44^{+0.13}_{-0.12}$	-19.271 ± 0.030
	r_d	[100, 300]	$148.6^{+7.5}_{-9.5}$	137.3 ± 2.3



Dynamical dark energy behaviour

But dark energy is dynamical!



Late-time limit ($z \rightarrow 1$)

$$\Omega_\Phi = 1$$

$$w_\Phi = -1, c_s^2 = 0$$

Intermediate times

$$\Omega_\Phi \rightarrow 0$$

$$-1 < w_\Phi < \frac{1}{3}, \quad 0 < c_s^2 < \frac{1}{3}$$

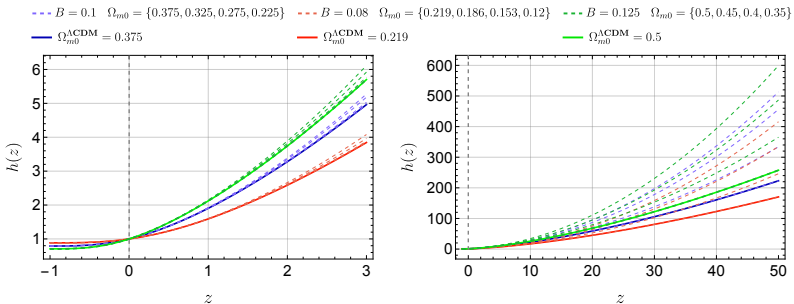
Early time limit ($z \rightarrow \infty$)

$$\Omega_\phi = 1$$

$$w_\Phi = \frac{1}{3}, \quad c_s^2 = \frac{1}{3}$$

Matter degeneracy

- Ω_{m0} has insignificant effect on low- z evolution



- k -essence field behaves like cosmological constant + matter contributions at late times (Scherrer 04')
- Full analytic solution and $z \rightarrow -1$ approximation confirm this behaviour

Parameter degeneracy

<i>k</i>-essence model	Parameter	Prior	JOINT	$\chi^2_{\text{tot,min}}$	AIC	BIC
$\Omega_{m_0} = 0$	H_0 \mathcal{M} r_d B	[50, 100] [-20, -18] [100, 300] [0.0625, 0.1666]	67.3 ± 3.9 -19.44 ± 0.13 $148.5^{+7.5}_{-9.6}$ $0.0921^{+0.0015}_{-0.0017}$	1778.70	1786.70	1808.52
$\Omega_{m_0} = 0.1$	H_0 \mathcal{M} r_d B	[50, 100] [-20, -18] [100, 300] [0.0694, 0.1708]	67.3 ± 3.9 $-19.44^{+0.13}_{-0.12}$ $148.5^{+7.6}_{-9.4}$ $0.0923^{+0.0015}_{-0.0018}$	1779.03	1787.03	1808.85
$\Omega_{m_0} = 0.2$	H_0 \mathcal{M} r_d B	[50, 100] [-20, -18] [100, 300] [0.0781, 0.1748]	67.3 ± 4.0 $-19.44^{+0.13}_{-0.12}$ $148.5^{+7.7}_{-9.6}$ $0.0925^{+0.0015}_{-0.0017}$	1779.26	1787.26	1809.08
$\Omega_{m_0} = 0.29$	H_0 \mathcal{M} r_d B	[50, 100] [-20, -18] [100, 300] [0.0880, 0.1784]	67.3 ± 3.9 $-19.44^{+0.13}_{-0.12}$ $148.6^{+7.5}_{-9.5}$ $0.0925^{+0.0015}_{-0.0018}$	1779.36	1787.36	1809.18
$\Omega_{m_0} = 0.303$	H_0 \mathcal{M} r_d B	[50, 100] [-20, -18] [100, 300] [0.0896, 0.1788]	67.3 ± 3.9 $-19.44^{+0.13}_{-0.12}$ $148.5^{+7.6}_{-9.6}$ $0.0927^{+0.0013}_{-0.0018}$	1779.37	1787.37	1809.19

Table 1: Constraints and fit statistics for geometric *k*-essence models with fixed Ω_{m_0} values.

Parameter degeneracy

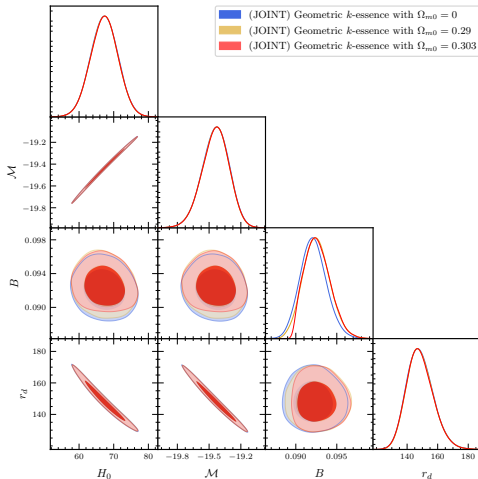


Figure 6: Corner plots showing the posterior constraints on the model parameters for the geometric k -essence model for different fixed values of Ω_{m0} .

- 1 Geometrical preliminaries**
- 2 Geometric k-essence**
- 3 Cosmological dynamics of geometric k-essence**
- 4 Late-time observational constraints**
- 5 Outlook**

Summary

- Geometric motivations and well-defined action principles
- Equivalence with well-known k -essence models
- Surprisingly, never been constrained before: due to phase space instabilities and parameter degeneracy
- Dynamical systems analysis used to inform priors
- Shown to be observationally indistinguishable from Λ CDM with late-time data
- Many follow-up directions

